Image Processing of Aluminum Alloy Weld pool for Robotic VPPAW based on Visual Sensing

Chun Jiang, Fubiao Zhang, Zhenmin Wang

***Abstract*—The intelligent welding technology is one of key development directions in "Industry 4.0" systems, and the use of sensing method is the main research direction of future intelligent welding technology. Due to the characteristics of aluminum alloy variable polarity plasma arc welding (VPPAW), by employing a complementary metal oxide semiconductor (CMOS) welding camera with a composite filter glass, a clear image of weld pool can be captured by side vision sensor. Aiming at the images captured with digital graphic processing technique, in this study images are processed by Labview vision module. Moreover, in this paper, a method for image processing, which includes reversing, local threshold determination based on variance within the group, Fast Fourier Transform (FFT) low-pass truncate filtering and advanced morphological operations for particle, is proposed to extract the characteristics of weld pool width. The result has shown that proposed image processing system can obtain reliable information on width of weld pool, which represents the basis for realization of quality control in aluminum alloy variable polarity plasma arc welding.**

***Index Terms*—Aluminum alloy, image processing, Industry 4.0，variable polarity plasma arc welding, vision sensing.**

I. INTRODUCTION

In the 21st century, the wireless sensor networks, large data, cloud computing and mobile Internet are rapidly entering the industrial manufacturing, bringing the entire industrial production system to a new level and driving a new industrial revolution. Namely, German technical academy and other institutions have jointly proposed the "The fourth generation of industry - Industry 4.0" strategy, designed to ensure the future competitiveness of German manufacturing industry and to lead the world industrial development trend[1-3]. The other major industrial countries have proposed similar strategies, such as "Industrial Internet" (US) and "Internet +" (China). The Industry 4.0 describes a production oriented Cyber Physics System (CPS), which combines production facilities, warehousing systems, logistics, and even social needs in order to create a global value creation network[4-6].

This work was supported in part by the National Natural Science Foundation of China under Grant 51375173, in part by the Science and Technology Project of Guangdong Province under Grant 2014B010104002 and Grant 2016B090927008, and in part by the Fundamental Research Funds for the Central Universities under Grant 2015ZP039.

School of Mechanical and Automotive Engineering, South China University of Technology, Guangzhou510640, China

Corresponding author: ZhenMin Wang (wangzhm@scut.edu.cn)

The Industry 4.0 is proposed to inject a new vitality into development of the manufacturing industry, and it tends to upgrade the global manufacturing intelligence, information technology and network technology. In the Cyber Physics System intelligent manufacturing development, welding technology is one of the indispensable parts of manufacturing industry, which is an important indicator of industrialization level, so the intelligent welding technology has become a hot topic[7]. The variable polarity plasma arc welding (VPPAW) has the advantages of small welding defects, good cathode cleaning effect, strong penetration ability and small deformation of workpiece[8]. The VPPAW has a potential application in intelligent manufacturing and fully meets the requirements of industrial development.

In the variable polarity plasma arc welding, the welding pool contains plenty of information, which is of great significance for welding automation control. At present, the main obstacles of the variable polarity plasma arc welding visual sensing are related to: shrink of plasma arc welding tungsten, big diameter of welding torch, short distance between welding gun and workpiece, and particularly narrow visual range of weld pool. At the same time, the arc compression energy concentration and strong arc resulting in greatly improved the difficulty of welding pool detection [9-12]. Since, the resistance of aluminum and aluminum alloy to the reflecting light and heat is high, the liquid surface color does not change significantly, thus the base metal and welding pool contrast is not obvious and detection of melting pool is more difficult, therefore studies on this subject are very rare. Zheng B and other scholars [13-15]chose the appropriate dimmer and filter to solve the problem of interference VPPAW arc to the certain extent, in order to get a part of weld pool and extract the geometry of weld pool and other information on weld pool. Luo M and other scholars[16-17] used a narrowband composite filter image sensing system to obtain the image part of keyhole weld pool from welding workpiece with positive detection and to extract the visible keyhole weld pool width and hole geometry information, but the quality of images and feature information accuracy need to be improved.

The abundant information obtained from the weld pool can be used to predict penetration, weld shape, weld defects, etc. Moreover, the skilled welders can predict and control the depth of penetration by observing the weld pool and visually inspecting the width of back weld. Liu Y K et al. used the adaptive neuro-fuzzy inference system (ANFIS) to simulate skilled welders, and to estimate the width of weld back using

This article has been accepted for publication in a future issue of this journal, but has not been fully edited. Content may change prior to final publication. Citation information: DOI 10.1109/ACCESS.2017.2761986, IEEE Access

the characteristic parameters of weld pool [18]. Huanwei Yu and et al. collected the arc spectral and visual information on the Al–Mg alloy pulsed GTAW process. In[19], the principal component analysis was utilized for spectral line identification, redundancy removal and spectral characteristic signals extraction. Then, the relationship between penetration status for different welding conditions and the corresponding signal spectra were discussed and clarified. Finally, a fuzzy system based on the signal spectra was developed and successfully used to estimate the percentage index of the weld penetration status. In recent years, the three-dimensional visual sensing method based on structural laser graphics has become the mainstream in weld pool geometry measurement. WJ Zhang et al. performed the GTAW strong arc real-time measurement for the mirror three-dimensional (3D) surface of weld pool[20], and established the model for welding parameters control by observing the 3D pool[21]; and after determination of the basic spatial relation between welding torch and helmet, and detailed analysis of the weld pool, they presented a new real-time 3D reconstruction algorithm for the surface of weld pool[22].

On the basis of previous research [23-26], this paper further studies the image processing of aluminum alloy weld pool for variable polarity plasma arc welding. The previously mentioned studies did not consider the reflection from aluminum alloy, which causes a strong interferes edge extraction of weld pool, and all mentioned algorithms are sensitive to noise and have poor anti-interference ability. Therefore, in this paper, a suitable passive visual sensing system is constructed, and clear images of weld pool are captured and then processed by Labview. Moreover, a method that has better image processing performances than existing algorithms is proposed to obtain clear and complete edge of weld pool, and it is based on reversing, local threshold determination based on variance within the group, Fast Fourier Transform (FFT) low-pass truncate filtering and advanced morphological operations for particle. Besides, it provides de-noising and has strong anti-interference ability. In addition, the melting width information on weld pool is obtained by curve fitting presented in [27], which provides the basis for establishment of the VPPAW penetration control model.

II. TEST SYSTEM

The VPPAW weld pool detection system based on passive vision is shown in Fig 1. As it can be seen in Fig. 1, test system included VPPA welding power source, wire feeder, ABB robot, control PC and visual sensor system. The visual sensor system consisted mainly of CMOS camera, UV chip, and filter. Because of the characteristics of aluminum alloy VPPAW arc spectrum, the filter system consisted of UV chip and narrowband filter (the center wavelength was 635nm, and the bandwidth was 15nm). In the experiment, the flat surfacing method was used, the speed of image acquisition of CMOS camera was 40 frames/s, the aperture was 8, and the resolution of camera was 1280×1024px. The CMOS camera was placed along the welding direction on the top of artifacts at weld pool side at shooting distance of 360mm. The angle between camera and workpiece surface was set to 20 °angle in order to avoid plasma arc welding gun block as far as possible, and to get a clear image of weld pool.

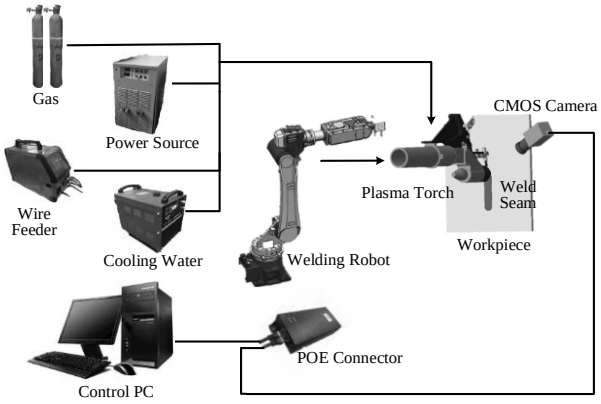

Fig. 1. Test system setup.

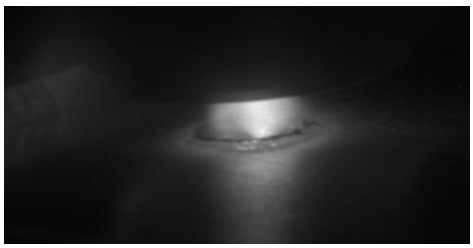

Fig. 2. Original pool image.

Using the presented test system, the weld pool image of vertical VPPAW of 6-mm plate was obtained. The welding parameters are shown in Table I, and the weld pool image is shown in Fig. 2.

TABLE I
WELDING PROCESS PARAMETERS

Positive current (A)	Negative current (A)	Positive and negative pole duty ratio	Plasma gas flow rate (L/min)	Welding speed (mm/s)
150	190	82:18	0.8	2.5

III. IMAGE PROCESSING AND EDGE EXTRACTION OF WELD POOL

The ultimate goal of the bath image processing is to detect the edge of VPPAW pool, and to obtain the geometrical parameters of weld pool. The quality control of VPPAW process is generally realized by detection of change of melting width, melting length and melting area in order to obtain an excellent weld.

Using the traditional filtering and image enhancement for preprocessing of weld pool image, the edge of weld pool was extracted by six edge detection operators. The result is shown in Fig. 3. According to the test results, six traditional edge detection operators do not accurately extract the edge of weld pool, and cannot dispose the impact of noise. In addition, there are many breakpoints at the weld pool edge, and extraction accuracy is not satisfactory. By comparing and analyzing these six detection operators, it can be concluded that the Laplacian operator has a relatively good detection performance, but it is hard to extract the geometric parameters of weld pool.

This article has been accepted for publication in a future issue of this journal, but has not been fully edited. Content may change prior to final publication. Citation information: DOI 10.1109/ACCESS.2017.2761986, IEEE Access

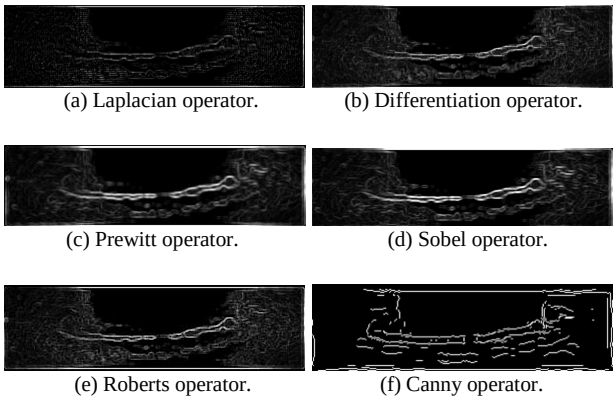

(a) Laplacian operator. (b) Differentiation operator.

(c) Prewitt operator. (d) Sobel operator.

(e) Roberts operator. (f) Canny operator.

Fig. 3. The edge detection results obtained by different edge operators.

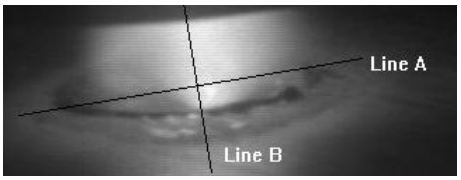

Fig. 4. Straight position.

Due to the high energy and arc concentration of variable polarity plasma arc welding, the CMOS camera was subjected to strong arc interference during the acquisition of weld pool image. As already mentioned, the traditional method based on spatial domain image processing cannot extract a satisfactory weld pool profile. Therefore, here the FFT low-pass truncate filter in frequency domain was used instead of the median filter in spatial domain to eliminate the noise interference. The straight position went through the arc center and followed the direction which is parallel to line A and vertical to line B, as shown in Fig. 4. The grayscale diagrams of line A and line B are shown in Fig. 5 and Fig. 6, respectively.

In Fig. 5(a), the original unprocessed grayscale diagram of line A is presented, and as it can be seen there is some noise on the line, and the curve is not smooth. After median filtering, the image is improved, Fig. 5(b). Using the FFT low-pass truncate filter instead of the median filter, the weld pool image is further improved. As it is shown in Fig. 5(c), the area between 1 and 2 is a solidified bead whose gray value is between 55 and 125, and its gray value is between the gray values of weld pool area and base metal area. Between 2 and 3, and between 4 and 5, the gray value is between 125 and 200, and that is the weld pool area. The peak between 3 and 4 is the bright arc area, where the gray value reaches the maximum in the whole image. In the area between 5 and 6 the grey value falls sharply. In addition, there is no clear weld pool area, which is due to the rapid forward movement of the heat source and reflection from the aluminum alloy during the variable polarity plasma arc welding. Of both point 6, which is on the right side, and point 1, which is on the left, the gray value is less than 55, which means that these areas represent the base metal area.

On the other hand, the original gray distribution of line B is presented in Fig. 6(a), wherein two hump areas can be noticed, one where the gray values are greater than 225 (arc area), and another where the gray values are about 150 (weld pool area).The gray values of adjacent pixels fluctuate greatly, but they are significantly improved by median filtering, Fig. 6(b).However, the fluctuation interference is effectively removed by FFT low-pass truncate filtering, Fig. 6(c).

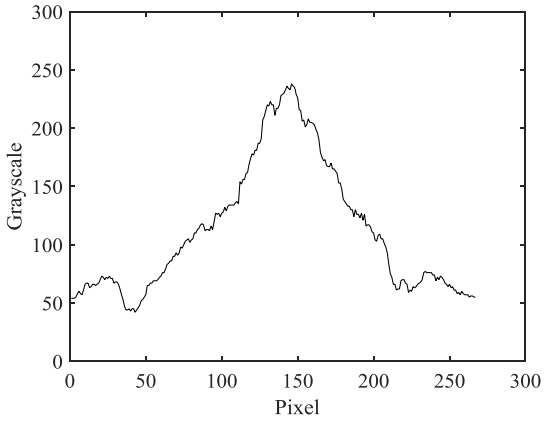

(a) Grayscale of straight line A.

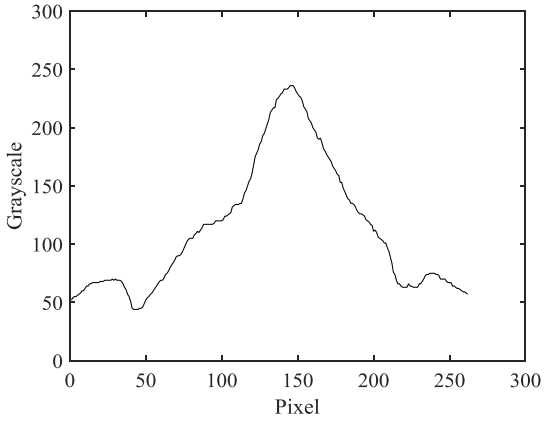

(b) Grayscale of line A after using median filter.

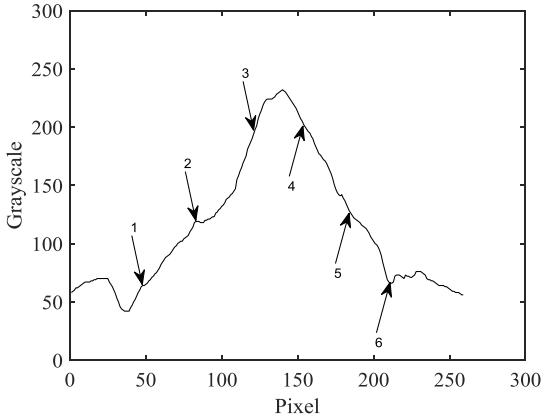

(c) Grayscale of line A after using low-pass truncate filter.

Fig. 5. Grayscale distributionof line A.

The images, histograms, and spectra after median filtering and FFT low-pass truncate filtering are shown in Fig. 7. In Fig. 7, it can be seen that median filter can improve histogram of the image and can eliminate isolated noise for partial gray values greater than 230 and less than 20. However, after using the median filter the spectrum is not very different, and the interference still exists in the weld pool image. On the other

This article has been accepted for publication in a future issue of this journal, but has not been fully edited. Content may change prior to final publication. Citation information: DOI 10.1109/ACCESS.2017.2761986, IEEE Access

hand, after using the FFT low-pass truncate filter noise interference is removed effectively, gray dynamic range is further compressed, and image smoothness is increased.

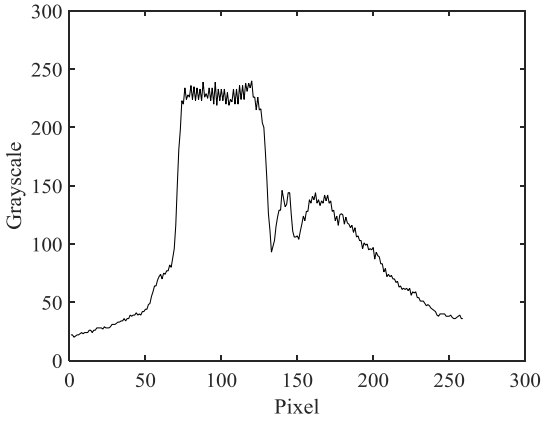

(a) Grayscale of straight line B.

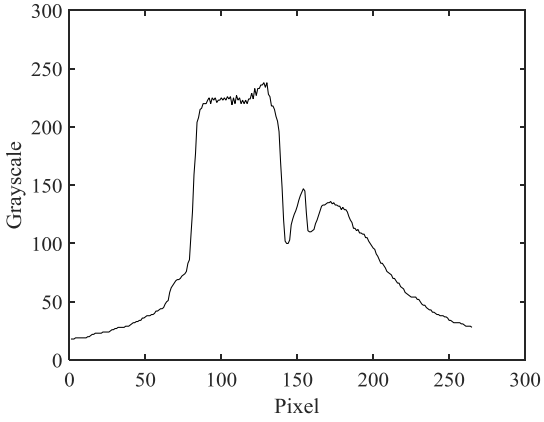

(b) Grayscale of line B after using median filter.

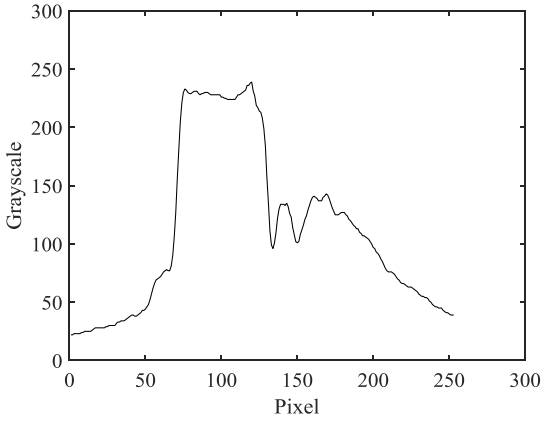

(c) Grayscale of line B after using low-pass truncate filter.

Fig. 6. Grayscale distributionof line B.

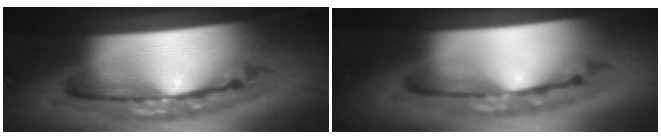

(a) Original image. (b) Image after using median filter.

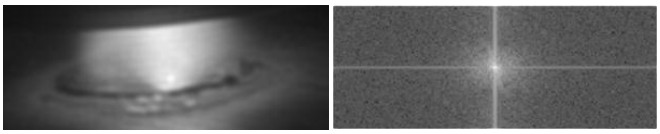

(c) Image after using low-pass truncate filter. (d) Spectrum after using median filter.

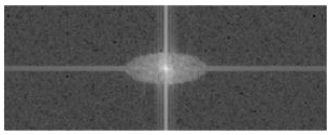

(e) Spectrum after using low-pass truncate filter.

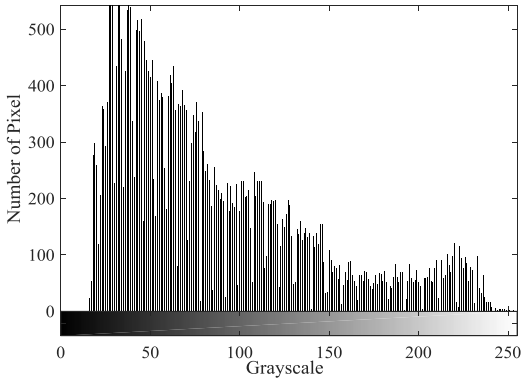

(f) Grayscale histogram of original image.

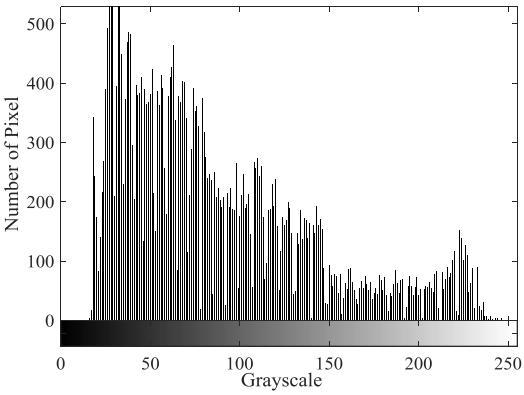

(g) Grayscale histogram after using median filter.

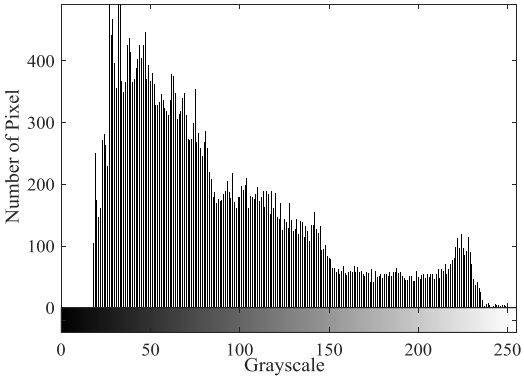

(h) Grayscale histogram after using low-pass truncate filter.

Fig. 7. Comparison of median filter and low-pass truncate filter.

Nevertheless, in the weld pool image spectrum diagram, there is still reflection, and the center circular area, which is a low frequency area, is surrounded by black high-frequency area, which shows a significant effect of FFT low-pass truncate filter on image processing of the weld pool for VPPAW.

The noise in the weld pool image usually corresponds to the high frequency part of Fourier transform, so the weld image smoothing and de-nosing can be achieved by attenuation of high frequency components in frequency domain. Besides, the image is usually taken by joint action of illumination and reflection from the target. Therefore, the image spectrum contains two parts of energy, part from illumination, and part from reflection. The spectrum energy of illumination is predominantly concentrated in the low-frequency band, while the energy of reflection is mainly concentrated in the middle and high frequency bands. The uneven illumination is mainly caused by reflection, and since the energy of reflection is mainly concentrated in the middle and high frequency bands, it has a little effect on the low-frequency part. Therefore, it is possible to suppress unevenness of the light by extracting the low frequencies from the spectrum. This shows that FFT low-pass truncation filter plays an important role in image acquisition of VPPA weld pool, which is beneficial to the subsequent image processing.

The advanced morphological operations are based on primary morphological operations and they are applied to the particles rather than to the pixels. The advanced morphological operations include filling of particles, removal of particles from the outside, removal of unwanted small or large particles, etc., and they are used to obtain the desired particles for quantitative analysis, observation of geometries, recognition of targets, etc. The experiments with advanced morphology of filled holes have shown that the desired processing of VPPAW weld pool images can be achieved. The vision module of Labview can be used to design the advanced mathematical morphology method for VPPAW weld pool image edge detection, and the main steps include: target area interception, image inversion, intra-group variance threshold determination, high-level morphological processing (removal of small particles, filling holes), FFT low-pass truncate filter processing and Canny edge detection. The processing flow is shown in Fig. 8, where the local threshold range for the black object based on intra-group variance is from 0 to 193, and the FFT low-pass truncation is defined by:

$$f_c = f_0 + a\%\left(f_{\max} - f_0 \right) \tag{1}$$

where f_c is the truncation frequency, f_0 is the minimal frequency of the signal(f_c=30.5Hz, f_0=20Hz), $f_{\max}$ is the maximal frequency of the signal, and a is the truncation rate, which is here equal to 5. Consequently, the spatial frequencies outside the truncation frequency range $\left[f_0, f_c \right]$ are removed.

The image edge can be smoothed by FFT low-pass truncate filter, thus the edge of the weld pool image can be obtained by image edge detection operator, which is beneficial to the feature extraction of weld pool geometry.

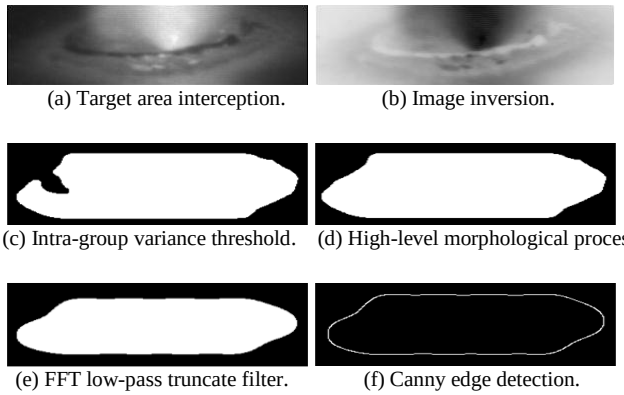

(a) Target area interception. (b) Image inversion.

(c) Intra-group variance threshold. (d) High-level morphological processing.

(e) FFT low-pass truncate filter. (f) Canny edge detection.

Fig. 8. Image processing of weld pool.

IV. EXTRACTION AND VERIFICATION OF WELD POOL WIDTH

The geometry of the weld pool mainly relates to the maximal width of weld pool, maximal length of weld pool, area of weld pool, and trailing angle. The maximal width of weld pool is defined as a maximal distance between two melting point boundaries vertical to the welding direction. In this study, the image processing algorithm is used to extract the width feature of weld pool, Fig. 9.

In order to verify the accuracy of visual system and image processing algorithm, measured values of weld width were compared with values obtained by image processing. Two main welding parameters including welding current and welding speed were selected, and they are listed in Table 2. While one parameter (welding current or welding speed) varied, the other was kept constant. The results are shown in Table II, wherein it can be seen that pool width increases when current increases from 150A to 170A. In addition, bigger current produces more heat, stronger arc and more molten metal, further,the increasing gravity and other forces make the molten metal to collapse, thus, more thermodynamic forces are applied along the depth direction, which results in bigger penetration and smaller weld width.

Meanwhile, it can be seen that weld pool width generally decreases with welding speed increase. In these processes, the heat input is certainly reduced resulting in lessening of weld pool. Nonetheless, it should be noted that there is a jump when welding speed is 2.75mm/s, which appears because the plasma arc is jetted from the keyhole. Therefore, the increasing welding speed may lower the penetration and changed the angle of the jetted arc.

TABLE II
COMPARSION OF MEASURED AND DETECTED POOL WIDTH

Positive current (A)	Negative current (A)	Weld speed (mm/s)	Actual weld seam width (mm)	Image detection width (mm)	Percentage of error (%)
150	190	2.50	9.54	9.62	0.84
160	190	2.25	10.27	10.50	2.24
160	190	2.50	9.79	9.98	1.94
170	190	2.50	9.97	10.22	2.51
160	190	2.75	8.91	9.14	2.58

This article has been accepted for publication in a future issue of this journal, but has not been fully edited. Content may change prior to final publication. Citation information: DOI 10.1109/ACCESS.2017.2761986, IEEE Access

In Table II, it is shown that there is a certain error between detected values obtained by image processing and measured values because the contrast between aluminum alloy in molten state and solid aluminum alloy is not obvious and the arc disturbance is strong. The error between measured and calculated data is less than 3%, therefore, the proposed image processing can accurately determine the actual weld pool width. Accordingly, the image processing algorithm presented in this paper is feasible and reliable.

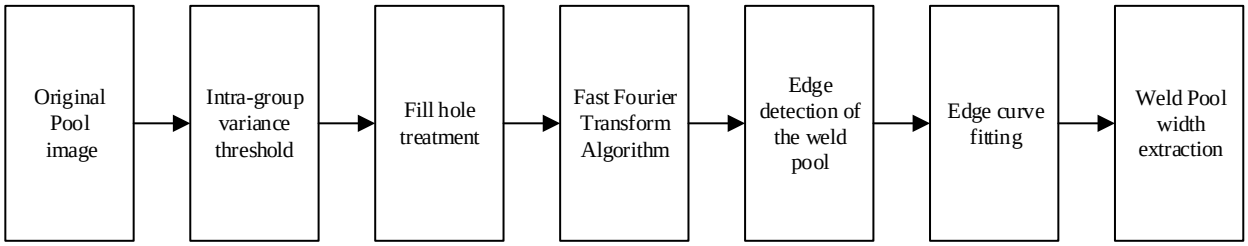

Fig. 9. Weld pool width extraction.

V. CONCLUSION

Using the variable polarity plasma arc welding characteristics of medium plate aluminum alloy, a clear weld pool image is obtained by a visual sensing system designed in this paper. The selection of appropriate light attenuator tablet and optical filter help to distinguish the weld pool and welding arc boundaries simultaneously. The image of the VPPAW weld pool is processed by advanced morphological operations and FFT low-pass truncate filter, and the edge of the weld pool image is obtained, thus, the noise disturbance is avoided. The edge curve fitting is performed on obtained weld pool image, and the weld pool width is tested to verify feasibility and accuracy of the proposed image processing algorithm.

According to the calculated values of weld pool width, the increase of welding current results in bigger penetration and smaller weld width, and the increase of welding speed results in smaller penetration and weld width.The presented low-cost visual sensing method provides an important possibility for Industry 4.0, wherein it can be used to predict and control the penetration as well as the keyhole status during the variable polarity plasma arc welding.

ACKNOWLEDGMENT

The authors declare that they have no conflict of interests.

REFERENCES

[1] M. A. Pisching, F. Junqueira, D. J. Santos, and P. E. Miyagi, "Service Composition in the Cloud-Based Manufacturing Focused on the Industry 4.0," in *Technological Innovation for Cloud-Based Engineering Systems*. vol. 450, L. M. CamarinhaMatos, T. A. Baldissera, G. DiOrio, and F. Marques, Eds., ed Berlin: Springer-Verlag Berlin, 2015, pp. 65-72.

[2] A. J. C. Trappey, C. V. Trappey, U. H. Govindarajan, J. J. Sun, and A. C. Chuang, "A Review of Technology Standards and Patent Portfolios for Enabling Cyber-Physical Systems in Advanced Manufacturing," *IEEE Access*, vol. 4, pp. 7356-7382, 2016.

[3] P. Haller and B. Genge, "Using Sensitivity Analysis and Cross-Association for the Design of Intrusion Detection Systems in Industrial Cyber-Physical Systems," *IEEE Access*, vol. PP, pp. 1-1, 2017.

[4] S. Wang, J. Wan, D. Li, and C. Zhang, "Implementing Smart Factory of Industrie 4.0: An Outlook," *International Journal of Distributed Sensor Networks*, vol. 2016, Article ID 3159805, 10 pages, 2016.

[5] X. Li, D. Li, J. Wan, A. V. Vasilakos, C. F. Lai, and S. Wang, "A review of industrial wireless networks in the context of Industry 4.0," *Wireless Networks*, vol. 23, no. 1, pp. 23-41, 2017.

[6] J. Wan, M. Yi, D. Li, C. Zhang, S. Wang, and K. Zhou, "Mobile Services for Customization Manufacturing Systems: An Example of Industry 4.0," *IEEE Access*, vol. 4, pp. 8977-8986, 2017.

[7] V. Tuominen, "The measurement-aided welding cell-giving sight to the blind," *International Journal Of Advanced Manufacturing Technology*, vol. 86, no. 1, pp. 371-386, Sep 2016.

[8] Y. F. Hsiao, Y. S. Tarng, and W. J. Huang, "Optimization of plasma arc welding parameters by using the Taguchi method with the grey relational analysis," *Materials And Manufacturing Processes*, vol. 23, no. 1, pp. 51-58, 2008.

[9] G. Zhang, C. S. Wu, and X. Liu, "Single vision system for simultaneous observation of keyhole and weld pool in plasma arc welding," *Journal of Materials Processing Technology*, vol. 215, pp. 71-78, 2015.

[10] Z. Liu, C. S. Wu, and J. Gao, "Vision-based observation of keyhole geometry in plasma arc welding," *International Journal of Thermal Sciences*, vol. 63, no. 63, pp. 38-45, 2013.

[11] Z. M. Liu, C. S. Wu, and M. A. Chen, "Visualizing the influence of the process parameters on the keyhole dimensions in plasma arc welding," *Measurement Science & Technology*, vol. 23, no. 10, p. 105603, 2012.

[12] C. S. Wu, L. Wang, W. J. Ren, and X. Y. Zhang, "Plasma arc welding: Process, sensing, control and modeling," *Journal of Manufacturing Processes*, vol. 16, no. 1, pp. 74-85, 2014.

[13] B. Zheng, H. J. Wang, and Q. L. Wang, "Front image sensing of the keyhole puddle in the variable polarity PAW of aluminum alloys," *Journal of Materials Processing Technology*, vol. 83, no. 1-3, pp. 286-298, 1998.

[14] H. Wang and R. Kovacevic, "On-line monitoring of the keyhole welding pool in variable polarity plasma arc welding," *Proceedings of the Institution of Mechanical Engineers Part B Journal of Engineering Manufacture*, vol. 216, no. 9, pp. 1265-1276, 2002.

[15] M. Luo and Y. C. Shin, "Vision-based weld pool boundary extraction and width measurement during keyhole fiber laser welding," *Optics And Lasers In Engineering*, vol. 64, pp. 59-70, Jan 2015.

[16] F. H. Shi, X. X. Huang, Y. Duan, and S. B. Chen, "Part-based model for visual detection and localization of gas tungsten arc weld pool," *International Journal Of Advanced Manufacturing Technology*, vol. 47, no. 9-12, pp. 1097-1104, Apr 2010.

[17] B. Guo, Y. H. Shi, G. Q. Yu, B. Liang, and K. Wang, "Weld deviation detection based on wide dynamic range vision sensor in MAG welding process," *International Journal Of Advanced Manufacturing Technology*, vol. 87, no. 9-12, pp. 3397-3410, Dec 2016.

[18] Y. K. Liu and Y. M. Zhang, "Model-Based Predictive Control of Weld Penetration in Gas Tungsten Arc Welding," *IEEE Transactions on Control Systems Technology*, vol. 22, no. 3, pp. 955-966, 2014.

[19] H. Yu, Z. Ye, and S. Chen, "Application of arc plasma spectral information in the monitor of Al–Mg alloy pulsed GTAW penetration status based on fuzzy logic system," *The International Journal of Advanced Manufacturing Technology*, vol. 68, no. 9-12, pp. 2713-2727, 2013.

[20] W. J. Zhang, X. W. Wang, and Y. M. Zhang, "Analytical real-time measurement of a three-dimensional weld pool surface," *Measurement Science & Technology*, vol. 24, no. 24, p. 5011, 2013.
[21] Y. K. Liu, W. J. Zhang, and Y. M. Zhang, "ANFIS modeling of human welder's response to three-dimensional weld pool surface in GTAW," *Journal of Manufacturing Science & Engineering*, vol. 135, no. 2, p. 021010, 2013.
[22] W. J. Zhang, J. Xiao, and Y. M. Zhang, "A mobile sensing system for real-time 3D weld pool surface measurement in manual GTAW," *Measurement Science & Technology*, vol. 27, no. 4, p. 045102, 2016.
[23] J. J. Yang, K. H. Wang, T. L. Wu, and A. M. Wei, *Image Feature Analysis of Weld Pool in Aluminium Alloy Twin Arc PMIG Welding Based on Snake Model*: Springer International Publishing, 2015.
[24] Y. Ogawa, "High speed imaging technique Part 1 – high speed imaging of arc welding phenomena," *Science & Technology of Welding & Joining*, vol. 16, no. 1, pp. 33-43, 2011.
[25] Z. Z. Wang, X. J. Ma, and Y. M. Zhang, "Simultaneous Imaging and Measurement of Pool Surface and Metal Transfer," *Welding Journal*, vol. 90, pp. 121S-128S, Jun 2011.
[26] X. G. Liu and B. Zhao, "Based on the CO2 gas shielded welding molten pool image edge detection algorithm," *Applied Mechanics & Materials*, vol. 437, no. 19, pp. 840-844, 2013.
[27] S. C. Juang and Y. S. Tarng, "Process parameter selection for optimizing the weld pool geometry in the tungsten inert gas welding of stainless steel," *Journal Of Materials Processing Technology*, vol. 122, no. 1, pp. 33-37, Mar 2002.